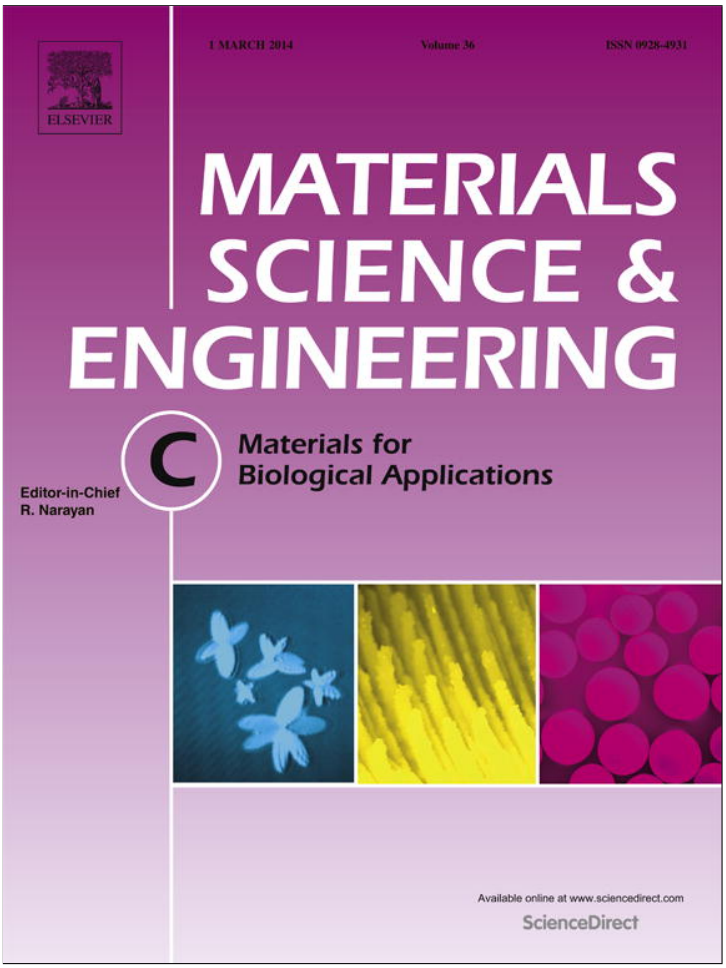

Materials Science and Engineering C 36 (2014) 108–117

Contents lists available at ScienceDirect

Materials Science and Engineering C

journal homepage: www.elsevier.com/locate/msec

Biopolymeric antimicrobial films: Study of the influence of hydroxypropyl methylcellulose, tapioca starch and glycerol contents on physical properties

Ricardo A. Espinel Villacrés [a], Silvia K. Flores [a,b], Lía N. Gerschenson [a,b,*]

[a] Industry Department, Natural and Exact Sciences School (FCEN), Buenos Aires University (UBA), Ciudad Universitaria, Intendente Güiraldes S/N, 1428 CABA, Argentina
[b] National Research Council (CONICET), Argentina

ARTICLE INFO

Article history:
Received 3 September 2013
Received in revised form 9 November 2013
Accepted 28 November 2013
Available online 10 December 2013

Keywords:
Edible films
Starch
HPMC
Potassium sorbate
Physical properties
Antimicrobial activity

ABSTRACT

Mixture design methodology was applied to study the effect of different levels of tapioca starch (TS), hydroxypropyl methylcelullose (HPMC), and glycerol (Gly) on the physical properties of biopolymeric films supporting potassium sorbate (KS; 0.3% w/w) with the goal of contributing to the development of materials for preventing food surface contamination. Mechanical properties, water vapour permeability (WVP), solubility in water (S) and colour attributes were evaluated on the films. HPMC addition produced an increase of elastic modulus (E_c), stress at break (σ_b) and S. It also decreased the yellow index (YI) values and the strain at break (ε_b).
The study was deepened using the formulation containing 2.67 g/100 g of TS, 0.67 g/100 g of HPMC, 1.67 g/100 g Gly and 0.3 g/100 g KS, observing that it behaved as an effective antimicrobial barrier against *Zygosaccharomyces bailii* external contamination. Microstructural analysis allowed us to conclude that HPMC incorporation to a TS network decreased roughness of the films and it also increased permeability to oxygen (PO_2).

1. Introduction

Biopolymeric edible films are useful for acting as barriers to gases (O_2, CO_2), water vapour, oils, solutes and volatile components and for helping in the separation of small pieces or portions of food for individual consumption. They can also improve mechanical properties and behave as active films while acting as reservoirs of food additives (antimicrobials or antioxidants) helping in food quality maintenance [1].

According to Campos et al. [2] the edible films can be manufactured with hydrocolloids or lipids. Hydrocolloids include proteins, cellulose derivatives, alginate, pectins, starches and other polysaccharides. The hydrocolloids constitute a tridimensional network or matrix capable of self-support and the lipids give flexibility to the films.

Starch is a storage polysaccharide for plants and it is the second most abundant biomass material in nature, cellulose being the first . Starch is also the principal source of energy in the human diet [3]. Edible films based on starch are odourless, tasteless, colourless, non-toxic and semipermeable to CO_2, resistant to O_2 and present physical characteristics that are similar to those of synthetic films [4].

Cellulose is a polysaccharide constituted by linear chains of D-glucose molecules linked by glucosidic β-1,4-O links. There are also observed hydrogen bonds between chains. Cellulose derivatives can be used to manufacture edible films that are resistant to lipids and strong. The hydroxypropyl methylcellulose (HPMC) is a cellulose derivative produced using propylene oxide and methyl chloride. It is a non-ionic polymer and its solutions are highly stable in the pH range 3–11. They are also resistant to high temperatures, being able to be extruded in the temperature range 120–190 °C when they are mixed with an adequate plasticizer like sorbitol or glycerol [5]. During the frying of meat, the use of HPMC coatings reduces the moisture loss and the oil absorption [4].

In general, the blend of different polysaccharides in adequate proportions is assayed for optimising the properties of the resultant biopolymeric film or for lowering the costs of the production of new materials with innovative properties to be used for specific purposes [6].

The objective of this research was: i) the development of biopolymeric edible films based on TS and HPMC using glycerol as plasticizer and potassium sorbate as antimicrobial, through a mixture design procedure; ii) the characterisation of the influence of film formulation on mechanical properties, solubility in water, colour and WVP; iii) the selection of formulations with good mechanical properties and low solubility and the characterization of these films by means of microscopy, and in relation to their oxygen barrier properties and antimicrobial performance.

* Corresponding author at: Departamento de Industrias, FCEN, UBA. Ciudad Universitaria, Intendente Güiraldes 2620. (1428) CABA, Argentina. Tel./fax: +54 11 4576 3366.
E-mail address: lia@di.fcen.uba.ar (L.N. Gerschenson).

0928-4931/$ – see front matter © 2013 Elsevier B.V. All rights reserved.
http://dx.doi.org/10.1016/j.msec.2013.11.043

2. Materials and methods

2.1. Description of experimental design

The methodology selected in the present work was a mixture design in which the proportions of different components of a blend were the independent factors and the sum of the proportions of the mixture components was always 1 [7]. Therefore, for a mixture of q components:

$$\sum_{i=1}^{q} x_i = x_1 + x_2 + \ldots\ldots + x_q = 1 \quad (1)$$

where x_i represents the proportion of the i^{th} component in the mixture.

Specifically, a three-component constrained mixture design with two overall centroid point replications (Table 1) was used to study the effects of interactions between ingredients on the physical performance of the films. The variables studied were the concentrations of TS, Gly and HPMC. The constrained limits of each component were determined in preliminary assays taking into account the characteristics of the films obtained in terms of flexibility, homogeneity and stickiness. The minimum and maximum levels of each mixture component were as follow: TS (2–3 g/100 g total system), HPMC (0–1 g/100 g total system) and Gly (1–2 g/100 g total system). The pseudocomponent values were calculated as: $P_{TS} = (C_{TS} - 2)/2$; $P_{HPMC} = (C_{HPMC} - 0)/2$ and $P_{Gly} = (C_{Gly} - 1)/2$; where P_i = pseudocomponent and C_i = real concentration of component. Fig. 1 shows a complete ternary diagram and the points on the triangle are the component proportions in the studied mixtures expressed as pseudocomponents according to Table 1. The films were characterised through the measurement of stress at break (σ_b), strain at break (ε_b), elastic modulus (E_c), solubility in water (S), water vapour permeability (WVP) and yellow index (YI).

A special cubic equation for three components was used to describe film behaviour in relation to its composition:

$$Y = \beta_1 X_1 + \beta_2 X_2 + \beta_3 X_3 + \beta_{12} X_1 X_2 + \beta_{13} X_1 X_3 + \beta_{23} X_2 X_3 + \beta_{123} X_1 X_2 X_3 \quad (2)$$

where Y is the measured response (σ, ε, S, WVP, YI), β's are the coefficients estimated for each linear and cross-product term of the model and X_1, X_2 and X_3 represent levels (expressed as pseudocomponents) of TS, HPMC and Gly, respectively. The positive values for the binary coefficients β_{ij}, indicate synergistic effects while the negative values represent antagonism. The analysis of variance (ANOVA) was used to examine the significance of the data fitting to the model (α: 0.05). The triangular contour plots generated from polynomial equation (Eq. (2)) for each response were accomplished using the software Statistica 6.0 for Windows (StatSoft Inc., USA, 2001).

Table 1
Three-component constrained mixture design.

Mixture	Original components (g/100 g total system)			Pseudocomponents		
	TS	HPMC	Gly	TS	HPMC	Gly
1V	3.00	0.00	2.00	0.50	0.00	0.50
2V	2.00	1.00	2.00	0.00	0.50	0.50
3V	3.00	1.00	1.00	0.50	0.50	0.00
4C	3.00	0.50	1.50	0.50	0.25	0.25
5C	2.50	1.00	1.50	0.25	0.50	0.25
6C	2.50	0.50	2.00	0.25	0.25	0.50
7C1	2.67	0.67	1.67	0.33	0.33	0.33
7C2	2.67	0.67	1.67	0.33	0.33	0.33
7C3	2.67	0.67	1.67	0.33	0.33	0.33

TS: tapioca starch, HPMC: hydroxypropyl metylcelullose, Gly: glycerol.

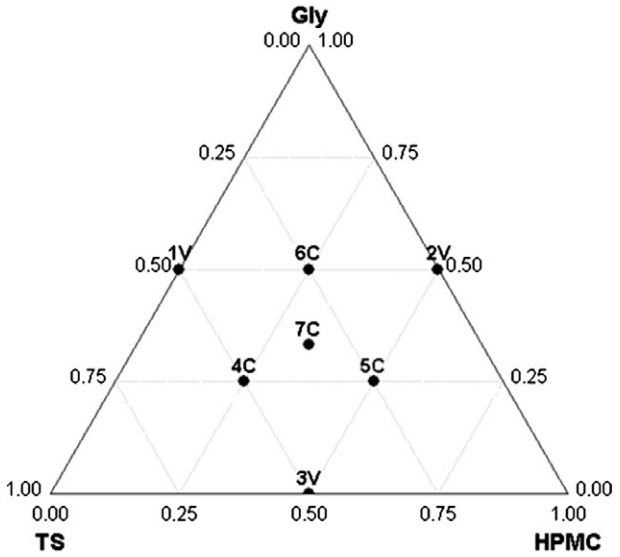

Fig. 1. Complete ternary diagram. Points included in the plot are the studied mixtures (Table 1). Component proportions are expressed as pseudocomponents.

2.2. Materials

The films were manufactured with cassava starch (Bernesa S.A., Argentina) and hydroxypropyl methylcellulose (Methocel Premium® K4M, Dow Chemical Co, USA). Glycerol (Sintorgan®, Argentina) was used as plasticizer. Antimicrobial agent included in the formulation was potassium sorbate, KS (Sigma®, USA).

2.3. Film preparation

HPMC aqueous solutions were heated under stirring (2.6 °C/min) to dissolution (final temperature: 82 °C). A suspension of TS in a gly-KS aqueous solution was added, under stirring, until total homogenization. Heating (0.8 °C/min) of the blend of hydrocolloids was performed under stirring to completely gelatinize the starch (final temperature: 82 °C). The tapioca starch and HPMC final contents are described in Table 1. For all tested formulations, the KS final concentration was maintained at 0.3% w/w. Vacuum was applied to each batch to remove air bubbles. After that, 20 g of these solutions were dispensed on Petri dishes (9 cm diameter) and the casting process was performed at 25 °C for 48 h. The films were removed from the plates and equilibrated at 57% relative humidity (R.H.), at 25 °C, before testing.

2.4. Physical properties

2.4.1. Mechanical characterization

The force (N)/displacement (mm) profile was evaluated through a tensile test on filmstrips (6 × 60 mm) mounted between the pneumatic grips of a Universal Testing Machine (Model 3345; Instron, USA). The initial grip separation and crosshead speed were set at 20 mm and 0.8 mm/s, respectively.

The stress ($\sigma = F/A$, being F the force and A the cross sectional area of the specimen; MPa) and the strain ($\varepsilon = H/L_0$, being H the crosshead displacement or extension of the sample and L_0, the initial effective length of the sample; %) were evaluated from the force/displacement profile. In particular, from the force (F_b) and extension at break (H_b), the stress (σ_b) and the strain at break (ε_b) were calculated. The elastic modulus (E_c) was evaluated from the initial slope of the true stress–true strain curve obtained from data fitting to the following exponential equation [8]:

$$\sigma_T(\varepsilon_T) = Ec \cdot \varepsilon_T \cdot \exp(\varepsilon_T \cdot K) \quad (3)$$

where σ_T and ε_T are the true stress and the true strain, respectively, being $\sigma_T = \sigma(1 + \varepsilon)$ and $\varepsilon_T = \ln(L/L_0)$. L is the effective length of the sample and is calculated as $(L = H + L_0)$; E_c is the elastic modulus and K is a constant fitting parameter.

Nine specimens were tested for each sample and the mean value and standard deviation were reported.

2.4.2. Water vapour permeability

Water vapour permeability (WVP) of films was determined gravimetrically using a modified ASTM E96 [9] procedure. The permeation cell (acrylic cups) contained $CaCl_2$ (0% R.H.; 0 Pa water vapour partial pressure). The covered cell was placed in a R.H. (70%) controlled chamber (Ibertest, Spain) maintained at 25 °C (2300 Pa, water vapour partial pressure). After 20–24 h, when the stationary water vapour transmission rate was attained, changes in the weight of the cell were recorded over a 4-day period and WVP was calculated.

2.4.3. Solubility in water

Solubility in water (S) is defined as the percentage of the dry matter in the film solubilized after 24 h of immersion in distilled water. Dry matter initial content (%) of the films was determined through the drying of 2 cm diameter discs in a vacuum oven at 100 ºC for 24 h. Other discs were cut, weighed and immersed in 50 ml of distilled water, with periodic stirring, for 24 h at 25 ºC. Non-solubilized films were taken out and dried (100 °C, 24 h) to determine the final dry matter content. Solubility was calculated as the ratio between the difference of the initial and final dry matter with respect to the initial dry matter content.

2.4.4. Colour evaluation

Film discs of appropriate diameter were rested on white background standard. Measurements were performed using a photocolorimeter (Minolta, Japan) with an aperture of 1.5 cm diameter. The yellow index (YI) was measured according to a standard test method (ASTM E1925 [10]) using a C illuminant and 2° observer. Fifteen measurements were performed for each sample.

2.5. Further study of the effect of HPMC incorporation to TS based films

Additional studies were performed to evaluate the effect of HPMC incorporation to TS based edible films.

2.5.1. Oxygen permeability

The oxygen permeability (PO_2) was determined according to ASTM 3985 [11], which is recommended for evaluation of thin film barrier properties. The equipment used was an Ox-Tran MS 2/61 (Mocon, USA). Before conducting the test, films were conditioned for 4 h at 23 °C and 0% RH. The oxygen concentration in the gas carrier was set to 21%. The operating temperature was 23 °C, nitrogen and oxygen gas flows were 10 cm^3/s and 20 cm^3/s respectively, and the measurement area was 10 cm^2. The reported value of O_2 transmission rate (OTR) corresponded to a concentration difference of 100% O_2 and a barometric pressure of 760 mmHg. The determinations were made in triplicate. For this, the film with the formulation 7C was used. Also a film with the same solid content as 7C but formulated only with starch was used.

2.5.2. Fourier transform infrared spectroscopy (FTIR)

Attenuated total reflection (ATR) assays with a resolution of 2 cm^{-1} were performed on the studied films using a spectrometer Spectrum V5.3.1 (Perkin Elmer, Inc., Massachusetts, USA). Spectra were obtained between 700 and 3700 cm^{-1} to identify the transmittance peaks for each formulation. For this, the film with the formulation 7C was used. Also a film with the same solid content as 7C but formulated only with starch was used.

2.5.3. Morphological characteristics: microstructure

Films with the formulation 7C and films with a total solid content identical to the one of 7C but only based on TS or HPMC, were studied with the purpose of clarifying the effect of HPMC presence on the microstructure.

2.5.3.1. Light microscopy. The films were cut in circles with a diameter of 1 cm, proceeding to the direct observation under the optical microscope (Axioskop 2 Plus; Zeiss, Germany).

2.5.3.2. Scanning electron microscopy. The microstructural analysis of the films was carried out by SEM. Film samples were maintained in a desiccator with P_2O_5 for two weeks to ensure that no water was present in the sample. To observe the cross-section, films were frozen in liquid N_2 and cryofractured. All samples were mounted on a bronze stub and sputter-coated (Cressington Scientific Instruments 108 Sputter Coater, United Kingdom) with a layer of gold prior to imaging. Micrographs of the film surface, as well as of its fracture surface, were obtained using a scanning electron microscope (SEM; Zeiss Supra 40, Germany) operated at an accelerated voltage of 10 kV.

2.5.3.3. Atomic force microscopy. The films were characterised using an atomic force microscope (AFM; NanoScope IIIa, Veeco, USA) using silicon nitride tips (V shape) with spring constant of 0.06 N/m. It was operated in "tapping mode" (TP-AFM) under nitrogen and topographical images were generated.

Three dimensional images were obtained by means of the Scanning Probe Microscopy programme (WSxM 4.0 Beta 1.1; Nanotec Electronica SL 2012, Spain).

Using the topographical data from AFM micrographs and the programme previously mentioned, roughness was evaluated. The average roughness (Ra) is the arithmetic mean of the deviations of the heights:

$$Ra = \frac{\sum_{i=1}^{N} Z_i - \overline{Z}}{N} \tag{4}$$

with

$$\overline{Z} = \sum_{i=1}^{N} \frac{Z_i}{N} \tag{5}$$

where Z_i is the height value (nm), $\overline{Z}$ is the arithmetic mean of the height (nm) and N is the number of observed points. The mean square roughness, Rq, has the following expression [12]:

$$Rq = \sqrt{\sum_{i=1}^{N} \frac{(Z_i - \overline{Z})^2}{N}}. \tag{6}$$

2.5.4. Antimicrobial effectiveness of films as barriers to yeast contamination

Films assayed were those of formulation 7C and TS films with the same solid content than the former with the purpose of evaluating the effect of HPMC presence on results obtained. Control films without KS were also formulated.

The antimicrobial activity of the films was evaluated using as indicator *Z. bailii*, a spoilage yeast known due to its resistance to several stress factors commonly used in food elaboration such as low pH, high levels of sugar, pasteurisation and, especially, addition of lipophilic preservatives. *Z. bailii* NRRL 7256 inoculum was prepared in Saboureaud broth at 25 °C until early stationary phase was achieved (24 h).

In order to study the performance of the films to prevent microbial contamination of a high water activity (a_w) product, a Saboureaud agar with a_w depressed to 0.980 by addition of glucose and pH adjusted to 4.5 with citric acid (5.2 mol/l) was formulated to resemble that kind

of products. Discs of 1 cm diameter were cut from films with or without KS and applied on the surface of the agar. Then, 10 μl of a culture of *Z. bailii* containing approximately 3–5 × 10^6 UFC/ml were seeded on the film discs. Samples were incubated at 25 °C for 48 h.

The sampling was performed at selected times by taking two discs and suspending each one in 1 ml of peptone water (Biokar Diagnostics, France) contained into a short glass tube. The samples were shaken for 2 min at 2500 rpm with a vortex (IKA-Works Inc., USA), prior to enumerating *Z. bailii* populations by surface plating on Saboureaud agar and incubation at 25 °C for 5 days.

3. Results and discussion

All films produced were homogeneous, flexible and transparent. Table 2 shows the value of mechanical parameters (σ_b, ε_b and Ec), S, YI and WVP for each film formulation (Table 1). Table 3 summarises the prediction equations that best fit ($p < 0.01$) to the measured responses and the lack of fit values ($P > 0.05$) for the predicted equations. The adjusted determination coefficients (R^2_{adj}), were in the range 0.9588–0.9846, suggesting that these models adequately predicted the observed responses. For a better understanding of the prediction equations, the ternary contour plots of the different responses evaluated were statistically generated. The analysis of the counter plots was performed considering the partial area of the triangle that represents the constrained mixture design under study (Figs. 1, 2a).

3.1. Mechanical characterization

Table 3 shows the equation that best fit the σ_b response as a function of the composition. It can be noted that the linear coefficient of HPMC was positive, while the linear coefficients of TS and Gly were negative, showing the reinforcing effect of the biopolymer HPMC and the plasticizing effect of glycerol. A synergistic effect between TS–HPMC and TS–Gly was also observed as well as a negative value for the coefficient of interaction (TS X HPMC X Gly). It is noteworthy that all the interaction coefficients were one order higher than those corresponding to the linear terms and, therefore, exerted a greater impact on the predicted response. Fig. 2b illustrates the contour plot of σ_b. It can be seen that an increasing proportion of Gly, contributed to the decrease of σ_b, while the increase of the proportion of HPMC determined a σ_b increase. The area corresponding to higher proportions of TS and Gly promoted the lowest stress values.

In the equation that modelled the dependency of the ε_b with the composition (Table 3), the corresponding linear HPMC coefficient was positive, while the linear coefficients of TS and Gly were negative. However, the binary interaction coefficient TS X Gly was positive and the ternary one negative, being both one order higher than linear coefficients. Fig. 2c shows that ε_b values increased as the TS and Gly proportions simultaneously increased, whereas the ε_b, in general, tended to decrease when the proportion of HPMC increased.

In the case of E_c equation, TS and HPMC linear coefficients were negative, whereas the Gly coefficient was positive but these coefficients were at least one order lower than significant interaction coefficients of the model. Therefore, E_c results were deeply influenced by the binary TS X HPMC coefficient (synergistic effect) and the ternary TS X HPMC X Gly (antagonistic effect). The E_c contour plot (Fig. 2d) shows that increasing the HPMC and decreasing the Gly ratios, the E_c response increased. On the other hand, for the levels studied, increasing the TS for higher Gly proportions, determined the diminishing of E_c.

According to the results obtained for mechanical properties, systems with a higher proportion of Gly showed the lowest σ_b and E_c values (Table 1). Probably, plasticisers could locate between the polymer chains, thereby reducing the cohesion of the film network and giving origin to a more flexible film structure [13,14]. On the other hand, systems with high HPMC:TS ratios promoted an increase of the tensile strength. These properties depend, to a large extent on the distribution and intensity of inter- and intra-molecular interactions. Apparently, by increasing the number of HPMC molecules, these interactions could be enhanced and, therefore, gave origin to a stronger matrix. Tian et al. [15] analysed the mechanical properties of biopolymer based edible films and suggested that it is possible to predict a crosslinking density (υ_e, mol/m^3) of the network structure using the Eq. (4) based on the theory of rubber elasticity which can be applied to some biopolymer matrices that develop a rubber like stress-strain pattern:

$$\upsilon_e = G/RT \tag{7}$$

where R is the universal gas constant (8.314 J/K mol), T is the absolute temperature (298 K) and G (MPa) is the shear modulus which describes the film plastic behaviour in a tensile assay. G can be extracted from the σ_T versus $\lambda^2 - 1/\lambda$ plot as the slope at the post-yield region, being $\lambda = \varepsilon_T + 1$, the strain ratio. The evaluation of υ_e for systems with a constant (TS + HPMC):Gly ratio and in the presence of KS (systems 1 V, 6C and 2 V) rendered values of 33.3, 235.0 and 732.4 mol/mol^3 for HPMC contents of 0, 0.5 and 1% w/w respectively, showing an increase of υ_e with the concentration of this polysaccharide. Probably HPMC promoted the development of a higher number of physical crosslinkings in the film increasing υ_e, helping to the good compatibility of the TS and HPMC biopolymer interfaces and influencing the tensile strength responses. Ghanbarzadeh et al. [16] studied the mechanical behaviour of carboxymethyl cellulose (CMC) and corn starch based edible films. These authors reported that the addition of CMC caused an increase in the film tensile strength of more than 59% in comparison to the pure starch films and without any significant decrease in the strain to break. This trend was attributed to the interfacial interaction between both polysaccharides due to their chemical similarity.

3.1.1. Solubility in water

The water solubility (S) is of great importance since it affects the potential uses of films. Some industrial applications may require a low solubility of these materials to ensure product integrity. In other cases, a high solubility of the films may be required for a properly product consumption.

Table 2
Responses obtained under the experimental design.

Mixture	σ_b (MPa)	ε_b	Ec (MPa)	S (%)	YI	WVP × 10^9 (g/m s Pa)
1V	0.2 ± 0.1	2.2 ± 0.3	0.13 ± 0.02	31 ± 2	11.5 ± 0.4	3.6 ± 0.4^{de}
5C	3.08 ± 0.6	0.4 ± 0.1	33 ± 4	59 ± 3	6.3 ± 0.5	2.8 ± 0.2^{bc}
4C	1.1 ±0.1	0.5 ± 0.1	10.4 ± 0.4	32 ± 4	7.0 ± 0.3	1.8 ± 0.2^{a}
3V	6.8 ± 0.6	0.45 ± 0.03	163 ± 8	46 ± 4	6.3 ± 0.4	2.3 ± 0.6^{ab}
6C	0.6 ± 0.1	0.52 ± 0.06	2.6 ± 0.1	49 ± 2	8.0 ± 0.7	3.0 ± 0.4^{cd}
7C1	2.0 ± 0.2	0.5 ± 0.1	16.0 ± 1.6	51 ± 7	6.2 ± 0.5	2.8 ± 0.2^{bc}
7C2	1.8 ± 0.2	0.5 ± 0.1	15.1 ± 1.5	42 ± 4	7.1 ± 0.5	1.9 ± 0.1^{a}
7C3	1.5 ± 0.2	0.49 ± 0.04	12 ± 1	50 ± 1	6.5 ± 0.4	3.1 ± 0.5^{cd}
2V	2.2 ± 0.4	0.55 ± 0.05	13.9 ± 1.7	56 ± 4	6.5 ± 0.4	3.72 ± 0.04^{e}

Values are the mean ± standard deviation. Values followed by the same letter do not differ significantly (α: 0.05). σ_b: Stress at break, ε_b: strain at break, E_c: elastic modulus, S: solubility in water, YI: yellow index, WVP: water vapour permeability.

Table 3
Prediction equations obtained under the experimental design.

Responses	Model	p	Lack of feet (P)	R^2_{adj}
σ_b	$Y = -7.35 \times TS + 5.37 \times HPMC - 1.06 \times Gly + 31.19 \times TS \times HPMC + 17.69 \times TS \times Gly - 74.92 \times TS \times HPMC \times Gly$	0.0002	0.0922	0.9846
ε_b	$Y = -0.86\ TS + 1.76\ HPMC - 0.70\ Gly + 11.78\ TS \times Gly - 24.15\ TS \times HPMC \times Gly$	0.0025	0.3111	0.9779
E_c	$Y = -94.51 \times TS - 53.94 \times HPMC + 87.54 \times Gly + 949.81 \times TS \times HPMC - 1955.60 \times TS \times HPMC \times Gly$	0.0001	0.0525	0.9872
S	$Y = -30.89 \times TS + 124.04 \times HPMC + 92.25 \times Gly - 209.92 \times HPMC \times Gly + 277.71 \times TS \times HPMC \times Gly$	0.0110	0.1109	0.9728
YI	$Y = 7.87 \times TS + 13.54 \times HPMC + 15.14 \times Gly - 17.88 \times TS \times HPMC - 31.59 \times HPMC \times Gly$	0.0012	0.8810	0.9588

σ_b: Stress at break, ε_b: strain at break, E_c: elastic modulus, S: solubility in water, YI: yellow index. The equations are written for pseudocomponent values.

Table 3 shows the best predictive equation for solubility. The Gly and HPMC linear coefficients were positive while the HPMC X Gly binary term was negative (antagonism). On the other hand, TS X HPMC X Gly ternary term was positive (synergism). In Fig. 2e, it can be observed that decreasing the proportion of HPMC and increasing the TS proportion, S diminished. This suggests that the addition of HPMC to starch films generated a matrix more susceptible to interaction with water. These results are consistent with those reported by Basch et al. [17] who reported S values ranging from 12 to 36% according to the HPMC:starch ratio (0:5, 0.5:4.5 and 1:4).

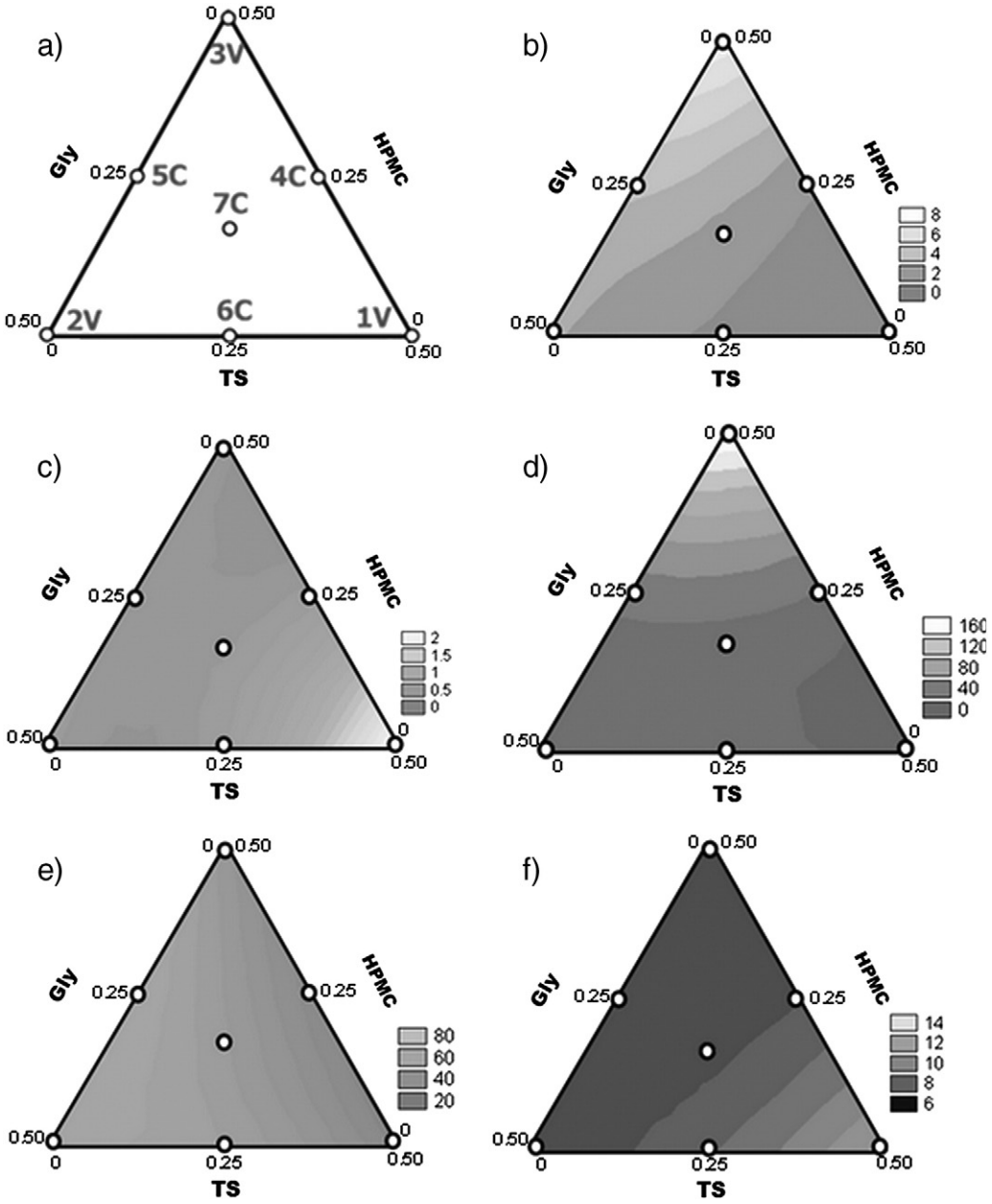

Fig. 2. Contours plots: a) location of systems from mixture design, b) stress at break (σ_b, MPa), c) strain at break (ε_b), d) elastic modulus (E_c, MPa), e) solubility in water (S,%) and f) yellow index (YI).

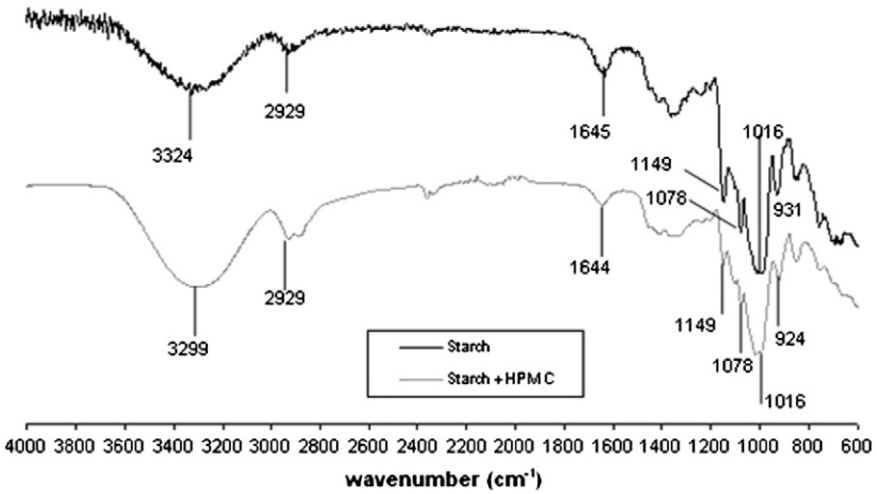

Fig. 3. FTIR spectra of TS and TS-HPMC based edible films.

According to the results obtained, it is possible to control the solubility of the TS/HPMC/Gly based films by changing the ratio of polymers used in their preparation.

3.1.2. Colour evaluation

The YI parameter is an evaluation of the yellowness associated to film visual appraisal, which is important regarding the consumer's acceptance. In general, it is desirable to have a low YI value to assure organoleptic acceptability.

The fitted equation (Table 3) shows that all linear coefficients were positive, while TS X HPMC and HPMC X Gly quadratic terms were negative (antagonistic effect). It can be seen in Fig. 2f that HPMC levels higher than 0.25 determined the lowest YI values independently of Gly and TS proportions, probably influenced by the strong effect of the interaction terms. However, for formulations with HPMC contents lower than 0.25, YI depended on the TS and Gly proportions, being higher as TS or Gly level increased. These results highlight that HPMC presence in the film formulation allowed the obtention of a less yellow matrix. Rotta et al. [18] studied the colour development of chitosan and HPMC based edible films, noting that the YI values were lower when the HPMC ratio was higher.

3.1.3. Water vapour permeability

In general, film thickness was around 0.22 ± 0.04 mm and this value was used for the calculation of the WVP. The WVP for the studied systems was in the range of 1.8×10^{-9} to 3.72×10^{-9} g/m s Pa (Table 2). Unfortunately, it was not possible to obtain a predictive equation in relation to WVP response for the mixture design, probably because many of the values obtained were not significantly different.

3.2. Effect of HPMC incorporation to tapioca starch based films

In order to analyse the effect of HPMC incorporation to tapioca starch based films, the following physical and structural characterizations were performed on films elaborated with the formulation 7C and its characteristics were compared with plane TS films with the same solid content.

3.2.1. FTIR

In order to elucidate potential interactions between starch and HPMC, FTIR spectra of the films without KS were evaluated. These interactions are often reflected as specific band shifts when a new ingredient is added to the formulation. Fig. 3 shows the FTIR-ATR spectra of TS–Gly and TS–HPMC–Gly based films. In the first case, it can be observed the starch characteristic bands at 931 and 1149 cm^{-1}, which are associated with the C–O bond stretching. The peaks at 1016 and 1078 cm^{-1} are characteristic of the C–O stretching anhydroglucose ring and the peak at 1645 cm^{-1} is due to O–H stretching of water molecules strongly coupled to the structure of starch. Another typical band is at 2929 cm^{-1}, which is associated with the C–H stretch of methine H atoms in the glucose ring. Finally, there is a broad band between 3100 and 3600 cm^{-1}, with a minimum at 3324 cm^{-1}, which is associated with the stretching of O–H groups either free, or attached via H bond intra- and intermolecular. When HPMC was incorporated into the film formulation, O–H and C–O bands appeared at lower wave numbers (3299 and 924 cm^{-1} respectively) suggesting that interactions were established between starch and HPMC. Probably, these interactions contributed to their compatibility and influenced the physical properties of these films.

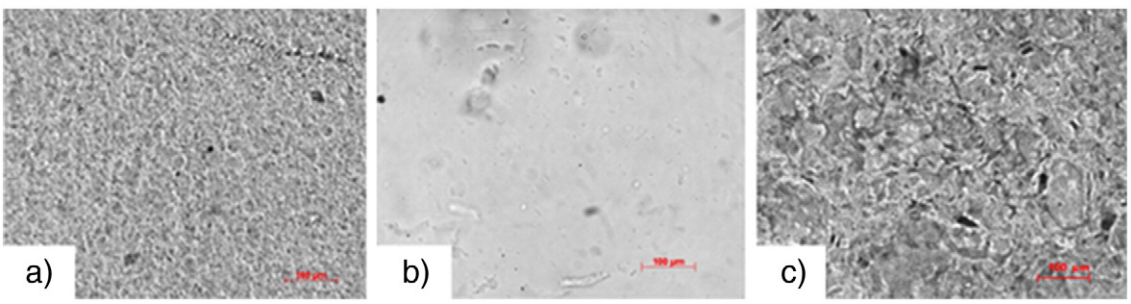

Fig. 4. Light microscopy of films elaborated from: Tapioca starch, TS (a), HPMC (b) and TS-HPMC (c). Magnification: 200×. Bar length: 100 μm.

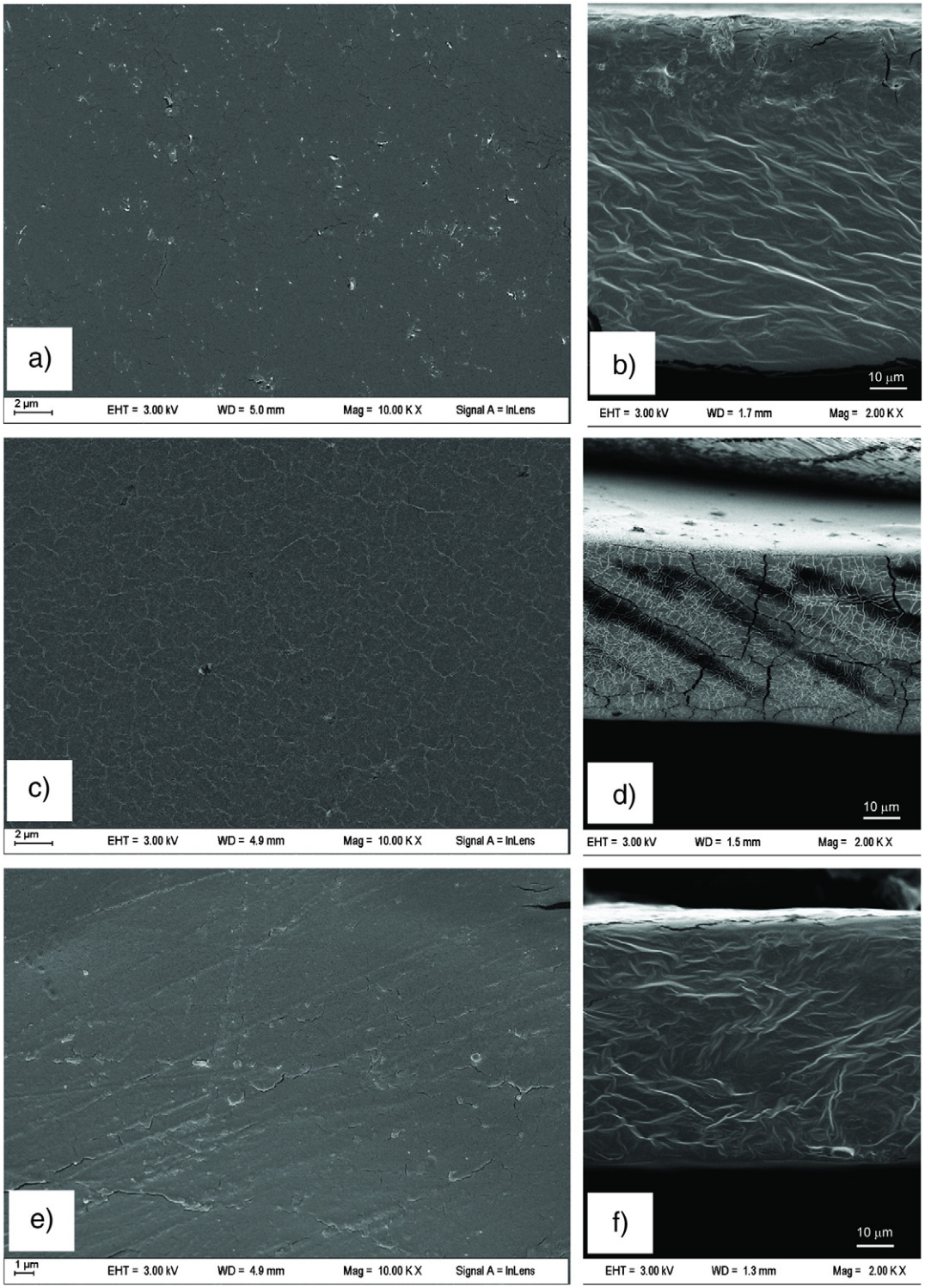

Fig. 5. SEM micrographs of films elaborated from: Tapioca starch (TS) film surface (a) and fracture surface (b), HPMC film surface (c) and fracture surface (d), TS-HPMC film surface (e) and fracture surface (f). Magnification: 10000× (surface) and 2000× (fracture).

3.2.2. Morphological characteristics: microstructure

3.2.2.1. Light microscopy. Fig. 4 shows the light microscopy images for the films formulated with TS or HPMC or TS–HPMC (7C). It is possible to observe that TS films (Fig. 4a) showed a continuous and uneven surface, rough, with grooves and presence of pores through which the solvent has evaporated during the drying process. HPMC films (Fig. 4b) were smoother and with some insolubilized cellulosic fibre fragments. TS-HPMC films (Fig. 4c) showed two separate phases, probably corresponding to a phase rich in starch and another one rich in HPMC, indicating that both biopolymers were intimately mixed but not solubilized one in the other. Morris [19] reported that systems formed by a binary blend of polysaccharides tended to form separate phases.

3.2.2.2. Scanning electron microscopy (SEM). Fig. 5 shows the SEM images of the surface and cross-sectional fracture surface of films studied. TS films (Fig. 5a) showed an irregular surface with many small spots

densely distributed in a continuous matrix. The cross-section surface of TS films (Fig. 5b) showed a sheet-like structure and as it advanced towards the solvent evaporation face, the matrix showed a distorted pattern.

HPMC films (Fig. 5c) presented a flatter surface which was organised in a block structure while its fracture surface (Fig. 5d) also exhibited a block structure with some air pockets, probably as an artefact of preparation procedure.

Blend biopolymer based films (system 7C) showed a surface with some irregularities (Fig. 5e) and a cross-sectional fracture surface with a sheet like structure, similar to TS film but less ordered (Fig. 5f) probably due to starch and HPMC chain interactions. This less ordered network might affect the optical and textural properties of the films.

It is important to remark that in all cases the structure was dense and compact suggesting a high structural integrity and good compatibility between the components.

Mali et al. [20] performed SEM observations of plasticized HPMC based films and detected a smooth surface without pores or cracks and a compact structure. These authors emphasised that a homogeneous

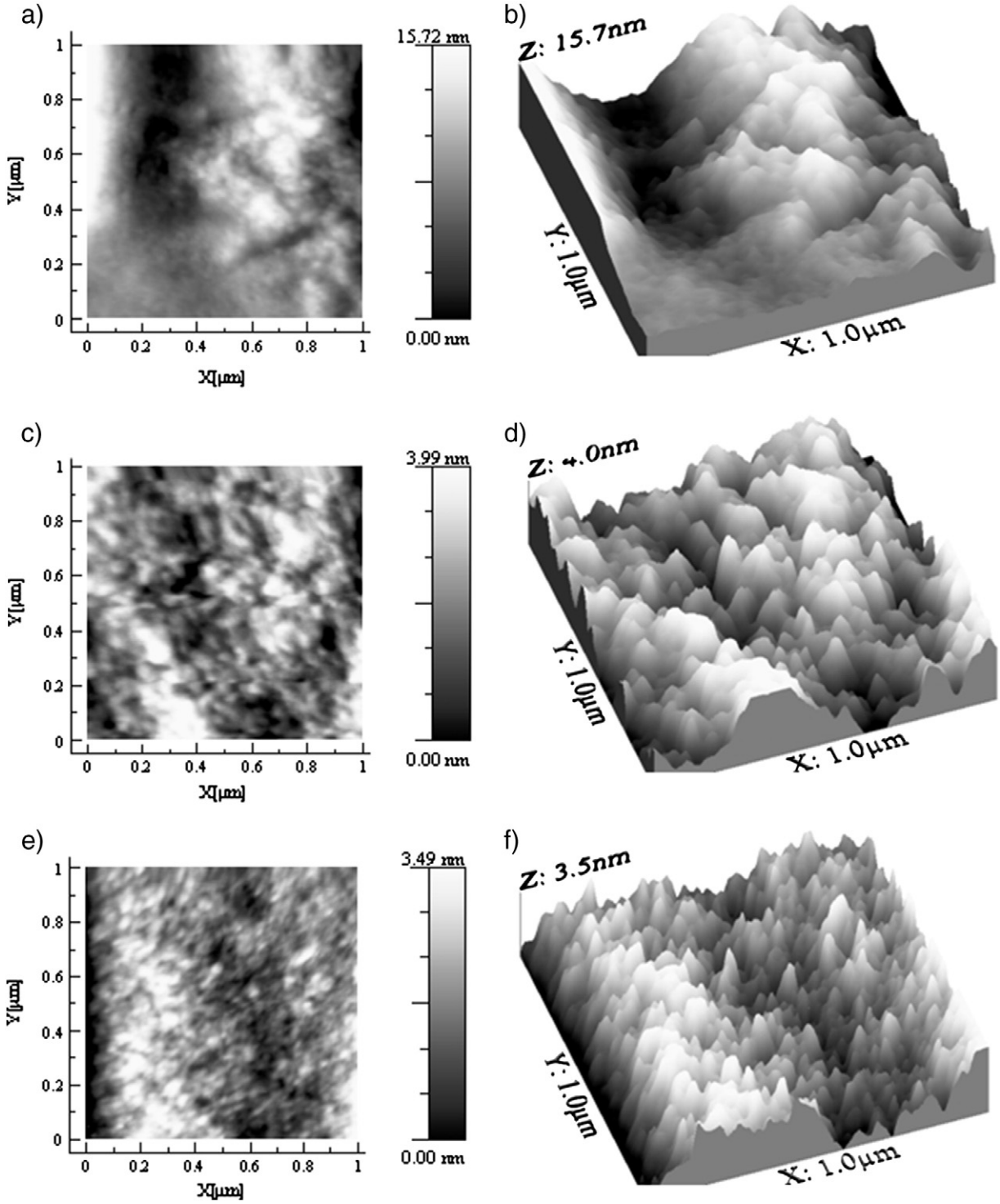

Fig. 6. TP-AFM images of films. Topographical: TS (a), HPMC (c), TS-HPMC (e) and three-dimensional: TS (b), HPMC (d), TS-HPMC (f).

film matrix is a good indicator of structural integrity and, therefore, of good mechanical properties.

3.2.2.3. Atomic force microscopy (TP-AFM). Film morphologies and roughness were analysed using TP-AFM. Fig. 6 shows the micrographs obtained from a scan area of 1 μm × 1 μm. As can be observed in the topographical and 3D micrographs for TS system (Fig. 6a and b), the surface was irregular with the presence of clusters of globular corpuscles (average diameter around 0.4–0.5 μm) and depressions. HPMC films (Fig. 6c and d) displayed abundant small granular structures (diameters ranging from 20 to 60 nm) with some aggregates of around 100 nm diameter. TS-HPMC films (Fig. 6e and f) showed a similar topography to HPMC based films and a dense population of thinner granules (10–30 nm) was noticed. It is important to remark that the heights of the structures in HPMC containing films were lower than the ones observed for TS based matrices. Rq and Ra parameters were determined in order to quantify the surface roughness of the films. TS based network had the roughest surface since Rq was 3.8 nm and Ra was 3.0 nm, while roughness parameters significantly diminished for HPMC films (Rq 0.95 nm and Ra 0.78 nm) and for 7C films (Rq 0.82 nm and Ra 0.66 nm). These values confirm qualitative results obtained from SEM images of film surfaces. Roughness might affect other film properties like optical ones.

3.2.3. Other properties

3.2.3.1. Permeability to oxygen (PO_2). The performance of films as a barrier to environmental oxygen was analysed. The PO_2 for TS films was $(1.2 \pm 0.2) \times 10^{-18}$ mol/m s Pa and this value is lower than those reported by other authors: 6.76×10^{-18} mol/m s Pa for corn starch based coatings measured at 24 °C [21] and 3.6 to 7.2×10^{-18} mol/m s Pa for potato amylose and amylopectin films at 23 °C [22] but it is important to state that the difference in the biopolymer used, composition of the formulation and technique of production, can affect the results.

In the present work, it could be observed that the HPMC incorporation (7C films) significantly increased the PO_2 to $(5.9 \pm 0.7) \times 10^{-18}$ mol/m s Pa with respect to TS films. It has been reported that films based on HPMC have PO_2 values of 127–330 $\times 10^{-18}$ mol/m s Pa [23]. Therefore, the blending of TS with HPMC produced a matrix with permeability values intermediate between those observed for matrices elaborated with each one of the pure hydrocolloids. It is important to remark that the studied films showed a lower PO_2 than the one reported for traditional packaging materials such as low density polyethylene (1003×10^{-18} mol/m s Pa) and polyvinyl chloride (16×10^{-18} mol/m s Pa).

3.2.3.2. Performance of edible films as antimicrobial barrier. The suitability of formulated films to act as a barrier against microbial contamination was evaluated using the yeast Zygosaccharomyces *bailii*. The "control" systems evaluated were formulated with TS or with TS and HPMC, in both cases, without KS.

Fig. 7 shows the microorganism growth with time, normalised to zero time. It can be observed that the yeast showed a 3 log cycle growth for both controls systems (TS and TS–HPMC films without KS) at the end of the storage. The TS–HPMC films supporting KS reduced the *Z.bailii* growth rate determining a final value that was 1.5 log cycles lower than the one observed for control systems. The decrease for TS films supporting KS was of, approximately, 0.8 log cycles. These results pointed out that KS supported in the films based on TS or on TS and HPMC, was available and that antimicrobial films studied constituted an effective barrier against external contamination by *Z.bailii*.

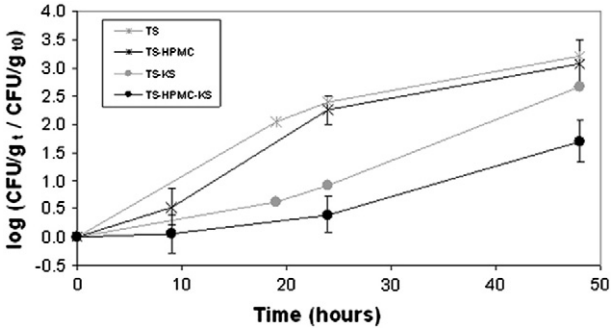

Fig. 7. Antimicrobial performance of TS and TS-HPMC films containing KS as a barrier against external *Z. bailii* contamination.

4. Conclusions

From the blend of tapioca starch, HPMC and glycerol it was possible to prepare uniform, transparent and easy handling edible films.

The application of experimental mixture design allowed us to obtain adequate prediction equations for the stress at break (σ_b), strain at break (ε_b), elastic modulus (E_c), solubility in water (S) and yellow index (YI). It could be concluded that an increase of HPMC content in the formulation produced a higher E_c and σ_b. The ε_b increased as the proportion of starch and glycerol were simultaneously increased. The water vapour permeability was not strongly influenced by the formulation, showing values between 1.8×10^{-9} and 3.7×10^{-9} g/m s Pa. The water solubility decreased as the content of starch increased. The yellow index of the films was lower when the amount of HPMC was higher.

The formulation containing 2.67 g TS, 0.67 g HPMC, 1.67 g Gly and 0.3 g KS per 100 g of system, showed good antimicrobial barrier properties against a *Z. bailii* external contamination of a semisolid food model (a_w 0.980 and pH 4.5), showing that KS was effective when supported in this biopolymeric matrix. The permeability to oxygen for this film was 5.9×10^{-18} mol/m s Pa, a value that is lower than the ones reported for synthetic films and it was observed that the HPMC presence tended to increase this permeability.

Microscopic examination showed that both biopolymers were intimately mixed but not solubilised in each other. There was a high structural integrity and good compatibility between the components of the blend and a roughness that decreased when HPMC was present, trends that could affect mechanical and optical properties of the films.

It can be concluded that active films based on tapioca starch and HPMC and supporting potassium sorbate could be formulated obtaining matrices with physical and functional properties compatible with their use to prevent the contamination of food surfaces. Additional studies in relation to their efficiency for controlling bacteria growth are being carried to completely characterise their functionality.

Acknowledgements

Authors acknowledge the financial assistance from Buenos Aires University (UBACyT 726); National Research Council of Argentina, CONICET (PIP 531); National Agency of Scientific and Technological Promotion of Argentina (PICT 2008 Number 2131).

References

[1] S. Min, J.M. Krochta, Antimicrobial films and coatings for fresh fruits and vegetables, in: W. Jongen (Ed.), Raw Material Safety: Fruit and Vegetables, Woodhead Publishing Ltd., Cambridge, UK, 2005.
[2] C. Campos, L. Gerschenson, S. Flores, Development of edible films and coatings with antimicrobial activity, Food Bioprocess Tech. 4 (2011) 849–875.
[3] J. Jay-lin, Starch: Structure and Properties, in: Chemical and Functional Properties of Food Saccharides, CRC Press, Florida, USA, 2004.
[4] C.N. Cutter, S.S. Summer, Application of edible coatings on muscle foods, Protein Based Films and Coating, CRC Press, Florida, USA, 2002.

[5] P. Mariscal, D.A. Bell, Fiber-based fat mimetics: methylcellulose gums, Handbook of Fat Replacers, CRC press, Florida, USA, 1996.
[6] G. Cazacu, V.I. Popa, Blends and composites based on cellulose materials, in: S. Dumitriu (Ed.), Polysaccharide: Structural Diversity and functional versatility, 2nd ed., Dekker, New York, USA, 2005.
[7] B. Barros Neto, I. Spacino Scarminio, R. Bruns, Como Fazer Experimentos, Pesquisa e Desenvolvimento na Ciência e na Indústria, Ed. Unicamp, Sao Paulo, Brazil, 2003.
[8] S. Chillo, S. Flores, M. Mastromatteo, A. Conte, L. Gerschenson, M.A. Del Nobile, Influence of glycerol and chitosan on tapioca starch-based edible film properties, J. Food Eng. 88 (2008) 159–168.
[9] ASTM E96, Standard test method for water vapor transmission of materials, Philadelphia: American Society for Testing and Materials, 2000.
[10] ASTM E1925, Standard test method for yellowness index of plastics, Philadelphia: American Society for Testing and Materials, 1995.
[11] ASTM 3985, Standard test method for oxygen gas transmission rate through plastic film and sheeting using a coulometric sensor, Philadelphia: American Society for Testing and Materials, 2002.
[12] B. Ghanbarzadeh, A.R. Oromiehi, Biodegradable biocomposite films based on whey protein and zein: barrier, mechanical properties and AFM analysis, Int. J. Biol. Macromol. 43 (2008) 209–215.
[13] S. Flores, D. Costa, F. Yamashita, L. Gerschenson, M. Grossmann, Mixture design for evaluation of potassium sorbate and xanthan gum effect on properties of tapioca starch films obtained by extrusion, Mat. Sci. Eng. C. 30 (2010) 196–202.
[14] S. Flores, L. Famá, A. Rojas, S. Goyanes, L. Gerschenson, Physical properties of tapioca-starch edible films: influence of filmmaking and potassium sorbate, Food Res. Int. 40 (2007) 257–265.
[15] H. Tian, G. Xu, B. Yang, G. Guo, Microstructure and mechanical properties of soy protein/agar blend films: effect of composition and processing methods, J. Food Eng. 107 (2011) (2011) 21–26.
[16] B. Ghanbarzadeh, H. Almasia, A.A. Entezami, Improving the barrier and mechanical properties of corn starch-based edible films: effect of citric acid and carboxymethyl cellulose, Ind. Crop. Prod. 33 (2011) 229–235.
[17] C.Y. Basch, R.J. Jagus, S.K. Flores, Physical and antimicrobial properties of tapioca starch-HPMC edible films incorporated with nisin and/or potassium sorbate, Food Bioprocess Tech. 6 (2013) 2419–2428.
[18] J. Rotta, R. Ávila-Ozório, A.M. Kehrwald, G.M. Barra de Oliveira, R. Dias de Melo, P.L. Manique-Barreto, Parameters of transparency, water solubility, wettability and surface free energy of chitosan/hydroxypropylmethylcellulose (HPMC) films plasticized with sorbitol, Mat. Sci. Eng. C. 29 (2009) 619–623.
[19] V.J. Morris, Polysaccharides: their role in food microstructure, in: D.J. McClements (Ed.), Understanding and Controlling the Microstructure of Complex Foods, Woodhead Publishing Ltd, Cambridge, UK, 2007.
[20] S. Mali, M.V. Grossmann, M.A. Garcia, M.N. Martino, N.E. Zaritzky, Microstructural characterization of yam starch films, Carbohyd. Polym. 50 (2002) 379–386.
[21] T.H. McHugh, J.M. Krochta, Milk-protein-based edible films and coatings, Food Technol. 48 (1994) 97–103.
[22] A. Rindlav-Westling, M. Stading, A.M. Hermansson, P. Gatenholm, Structure, mechanical and barrier properties of amylose and amylopectin films, Carbohyd. Polym. 36 (1998) 217–224.
[23] A. Jiménez, M.J. Fabra, P. Talens, A. Chiralt, Influence of hydroxypropylmethylcellulose addition and homogenization conditions on properties and ageing of corn starch based films, Carbohyd. Polym. 89 (2012) 676–686.